Published in final edited form as:
J Am Coll Cardiol. 2008 July 1; 52(1): 1–12. doi:10.1016/j.jacc.2008.03.036.

Radionuclide imaging - A molecular key to the atherosclerotic plaque

Harald Franz Langer, MD[1,*], **Roland Haubner, PhD**[2], **Bernd Juergen Pichler, PhD**[3], and **Meinrad Gawaz, MD**[1]

1*Medizinische Klinik III, Eberhard Karls Universität Tübingen, Germany; Dr Langer is currently affiliated with the Experimental Immunology Branch, National Cancer Institute, NIH, Bethesda, Maryland, USA*

2*Universitätsklinik für Nuklearmedizin, Medizinische Universität Innsbruck, Innsbruck, Austria*

3*Laboratory for Preclinical Imaging and Imaging Technology, Clinic of Radiology, University of Tübingen, Röntgenweg 13, 72076 Tübingen, Germany*

Abstract

Despite primary and secondary prevention, serious cardiovascular events like unstable angina or myocardial infarction still account for one third of all deaths worldwide. Therefore, identifying individual patients with vulnerable plaques at high risk for plaque rupture is a central challenge in cardiovascular medicine. Several non-invasive techniques, such as MRI, multislice computed tomography and electron beam tomography are currently being tested for their ability to identify such patients by morphological criteria. In contrast, molecular imaging techniques use radiolabeled molecules to detect functional aspects in atherosclerotic plaques by visualizing its biological activity. Based upon the knowledge about the pathophysiology of atherosclerosis, various studies *in vitro, in vivo* and the first clinical trials have used different tracers for plaque imaging studies, including radioactive labelled lipoproteins, components of the coagulation system, cytokines, mediators of the metalloproteinase system, cell adhesion receptors and even whole cells. This review gives an update on the relevant non-invasive plaque imaging approaches using nuclear imaging techniques to detect atherosclerotic vascular lesions.

Keywords

Plaque imaging; atherosclerosis; radionuclide imaging; vulnerable plaque; thrombogenicity

INTRODUCTION

Cardiovascular diseases are the most frequent causes of death in the western world and represent a central challenge for modern research and medicine. Rupture of the atherosclerotic plaque accounts for approximately 70% of fatal acute myocardial infarctions and/ or sudden coronary deaths (1). Thrombotic complications, which arise from rupture or erosion of a

*Corresponding author: Harald Langer, MD, Medizinische Klinik III, Eberhard Karls Universität Tübingen, Otfried-Muellerstr. 10, 72076 Tuebingen, Germany. At present affiliated with: NIH/NCI. Building 10, Room 4B17. Bethesda, MD 20892 E-mail address: E-mail: langerh@mail.nih.gov. 301-435-6468 (phone) 301-496-0887 (fax).

Conflict of interest: None.

vulnerable plaque, may be clinically silent yet contribute to the natural history of plaque progression and ultimately luminal stenosis (1). Therefore, it seems to be essential to acquire information beyond the resulting degree of stenosis detected by angiography. Over the past years, profound knowledge about the mechanisms involved in atherogenesis was obtained due to ambitious and excellent research. In the future, it is our responsibility to extend this knowledge by utilizing the field of molecular plaque imaging to obtain new strategies to detect vulnerable atherosclerotic plaques that cause critical cardiovascular complications.

The “vulnerable plaque”

To identify apparently healthy subjects at risk for future cardiovascular events a consensus of experts has recently defined criteria for the diagnosis of “vulnerable plaques” (1). Besides minor criteria like calcified nodules, yellow appearance of the plaque or intraplaque hemorrhage, major criteria have been established that represent different aspects of the rupture-prone plaque (Fig 1). Major criteria are active inflammation, thrombogenity and plaque injury. Further major criteria are related to plaque morphology and include a thin cap, a large lipid core or severe luminal stenosis. (1) Many groups have focussed on anatomic imaging modalities such as intravascular ultrasound, MRI, multislice computed tomography and electron beam tomography to view the vulnerable plaque (2–4).

Recent approaches using radionuclide imaging are based upon the pathophysiology of atherogenesis and have been evaluated to detect atherosclerotic lesions with a strong focus on the functional aspects of a plaque (Fig 2). The development of atherosclerotic plaques is a process of complex, consecutive and interacting steps involving chemokines, the upregulation of adhesion molecules, recruitment of inflammatory cells to the arterial wall, transmigration of these cells and the development of lipid-laden macrophages, (the so called foam cells), from invading monocytes (5). As a result of these processes, the early lesion of atherosclerosis - the fatty streak - appears. Subsequently, more complex lesions develop mediated by proliferation and migration of smooth muscle cells and excessive production of extracellular matrix proteins (5). Superficial erosions or fracture of the fibrous cap lead to plaque disruption followed by thrombus formation (6). Over the past years, distinct mediators and regulators involved in the cascade of atherosclerosis have been identified, which can be used to develop tools for the detection and characterization of atherosclerotic plaques by means of non-invasive molecular imaging (Table 1). The different approaches include radionuclide labelled lipoproteins (7), components of the coagulation system (8), cytokines (9), mediators of the MMP-system (10), cell receptors (11) and even whole cells (12). This review gives an update on the relevant non-invasive approaches in plaque imaging with a focus on radionuclide based techniques to detect vulnerable vascular lesions.

Nuclear imaging versus other non-invasive modalities to visualize the atherosclerotic plaque

Coronary angiography has so far been the gold standard to assess narrowing of the vessel lumen. Other invasive techniques have been introduced which provide additional information for plaque characterization, including intravascular coronary ultrasound, angioscopy, intravascular elastography, termography or optical coherence tomography. All these techniques have the disadvantage of being invasive. Towards the same end, increasing effort has been placed on non-invasive imaging techniques. The three major modalities used are magnetic resonance imaging (MRI), multislice computed tomography (CT) and nuclear imaging, each of them having advantages and disadvantages. In addition to stenosis detection, electron beam CT (EBCT), dual source (dual energy) and multislice CT (MSCT) are capable of picturing the coronary artery wall. By using MSCT, various components of the atherosclerotic wall may be distinguishable, allowing for identification of calcified areas or

hypodensities, which correlate to echolucent areas seen with IVUS (13,14). While such hypodense areas are suggestive of lipid-rich plaques, differential-diagnosis of such areas can include other tissue types such as less dense fibrous tissue. Thus, while providing a better spatial resolution than nuclear imaging techniques, CT based techniques may give less information on distinct plaque components aside from the level of calcification. Using MRI, T1 and T2-weighted imaging can provide *in vitro* information of the atheromatous core, collageneous cap and calcifications. (15) Although MRI provides good spatial resolution, results at the coronary artery level have not yet been convincing, as the arteries are small, tortuous vessels in continuous movement, which causes image aquisition difficulties. However, contrast-enhanced sequences have been tested and shown to improve the sensitivity of the method (16). CT and MRI mainly provide information based on morphology or anatomy.

The strength of nuclear imaging is its ability to provide quantitative information on a functional level such as density of a specific receptor or the metabolic activity of a plaque. Nuclear imaging is based on radiolabeled biomarkers with a signal sensitivity in the pico-molar range which is one million to one billion times above that of MRI or CT. Thus, nuclear imaging may be the most promising approach for vulnerable plaque detection. Currently, the leading modality in nuclear medicine is positron emission tomography (PET), which acquires images with a spatial resolution up to 4–5 mm, thereby improving on the performance of single photon emission computed tomography (SPECT), which has a resolution of 10–15 mm. To obtain good-quality images, the radiotracer must have rapid clearance from the bloodstream and a good target-to-background ratio. Given the small size of the plaque, in which the radionuclide concentrates, a high background signal can impair the quality of PET or SPECT images. Thus, the identification of promising highly specific molecular targets is of central importance. Another problem that complicates imaging of coronary arteries is related to vessel anatomy and heart pulsatility. Although the fast imaging protocols of MRI or CT are advantageous over the relatively slow PET or SPECT imaging, modalities such as cardiac gating can improve motion artefacts in cardiac imaging. Current research in imaging technology centers on the development of multimodality scanners, such as PET/CT or more recently PET/MRI, to provide comprehensive morphological and functional information during one scan session. Such technical advance, in particular PET/MRI, has enormous potential in the field of cardiac imaging as it allows for simultaneous data acquisition, which is a huge improvement compared to the sequential scanning protocols of PET/CT. Although these approaches do not improve spatial resolution of the PET technique, they provide valuable information about the localization of the aquired signal.

Radionuclide Imaging of Plaque

Metabolic Activity

Atherosclerotic plaques are characterized by an accumulation of cells with high metabolic activity. Therefore, various approaches addressed the principle of metabolic activity to image atherosclerosis. Strategies to find a feasible molecular target included the imaging of metabolically active cells, metabolic substrates or increased uptake of molecules in active cells. One of the earlier attempts to visualize atherosclerotic lesions used ^{111} In labelled patient derived monocytes, which were re-injected, and relied on the presumption that these monocytes become invasive plaque macrophages (17). A more practical way to image metabolically active macrophages and inflammation in general is the use of ^{18}F-radiolabled fluorodeoxyglucose (^{18}F-FDG). FDG competes with glucose for uptake into metabolically active cells such as macrophages. As it is already established in clinical practice to image tumors and myocardial viability and thus readily available, the use of FDG is an attractive strategy for imaging atherosclerotic lesions and several FDG based studies have been carried out. In one instance for example, a clinical study successfully employed autoradiography to visualize ^{18}F-FDG uptake in macrophage rich lesions of carotid endarterectomy specimen *ex vivo* (18).

A recently published study suggested the use of alternative tracers that operate on a similar principle, namely fluorocholine. ^{18}F-labeled fluorocholine (^{18}F-FCH) has been introduced as a tracer for imaging both brain and prostate cancers.

This Choline derivative is taken up into cells by specific transport mechanisms, phosphorylated by choline kinase, metabolized to phosphatidylcholine, and eventually incorporated into the cell membrane. (19,20) The increased choline uptake in highly proliferative cells such as tumor cells (21) and activated macrophages (20) has been related to an upregulation of choline kinase as well as an increased activity of cholinespecific transporters (21). Choline kinase expression and activity seems to be similar in normal and atherosclerotic murine aortae (22). Thus, enhanced ^{18}F-FCH uptake in activated murine plaque macrophages is not caused by changes in choline kinase, but rather by increased choline transport (22). The rapid uptake (within 30 minutes) of ^{18}F-FCH into inflammatory tissues supports this notion (23,24). To demonstrate the relative efficacy of ^{18}F-FCH versus^{18}F-FDG, Matter et al. injected apolipoprotein E-deficient mice intravenously with either tracer. *En face* measurements of aortae isolated 20 minutes after ^{18}F-FCH injections demonstrated a very good correlation between fat stainings and autoradiographies achieving a sensitivity of 84% to detect plaques while ^{18}F-FDG reached a lower sensitivity of 64% (22).

Chemotaxis

In the early atherosclerotic plaque, chemokines play an essential role, as they attract inflammatory cells to the lesion and keep the inflammation process progressing (5). One strategy to image atherosclerotic plaques is, thus, to visualize the expression of chemokines or their receptors within the vascular wall. Similarly to chemokines, adhesion receptors mediate the recruitment of inflammatory cells to the atherosclerotic plaque. Thus, potential imaging strategies are to visualize chemokines, chemokine receptors or adhesion receptors or ligands.

Monocyte chemoattracting protein-1 (MCP-1) is one of the strongest chemotactic agents, attracting inflammatory cells to the atherosclerotic plaque. (5,25) Although MCP-1 is not expressed in healthy vessels various stimuli (eg. tumor necrosis factor and other cytokines) can induce the expression and secretion of MCP-1 in endothelial cells, vascular smooth muscle cells or cardiomyocytes, which by triggering and sustaining leukocyte accumulation promotes inflammation (26). Elevated levels of circulating MCP-1 have been found in patients with congestive heart failure and coronary artery disease and have been adversely correlated with disease progression (27). Ohtsuki and colleagues analyzed the localisation of its receptor by using ^{125}I-MCP-1 (half-time ~ 10 min) in atheromas of cholesterol-fed rabbits 4 weeks after arterial injury of the iliac artery and the abdominal aorta. (9) The activity of ^{125}I-MCP-1 correlated with macrophage content per unit area as detected by immunohistochemistry using an antibody specific for rabbit macrophages. Furthermore, *ex vivo* autoradiography revealed high ^{125}I-MCP-1 activity within the vascular lesions. Along with chemotaxis, the upregulation of adhesion molecules on endothelial cells or leucocytes is also involved in atherosclerotic inflammation. Recently an established receptor ligand pair, VCAM-1 (endothelial cells) and VLA-4 (leucocytes) has been used to visualize atherosclerotic plaques (28,29). Using a novel VCAM-1 peptide affinity ligand identified by phage display that was conjugated to a magnetofluorescent nanoparticle, atherosclerotic plaques could be visualized by MRI as the ligand was actively internalized by VCAM-1 expressing cells (29). While the number and range of studies are limited, the use of chemokines may be a promising candidate for non-invasive plaque imaging in future clinical practice.

Angiogenesis/$\alpha_v\beta_3$ integrin

Accumulating evidence suggests that the extent of neovascularisation is closely linked to the inflammatory reaction and infiltration of macrophages/foam cells within atherosclerotic

plaques. A study of 269 advanced human atherosclerotic plaques concluded that micro vessel formation is strongly correlated with both plaque rupture and the signature features of vulnerable plaques. (30) So far noteworthy studies have used one molecular target involved in the angiogenesis process, the $\alpha_v\beta_3$ integrin. This integrin is a heterodimeric transmembrane glycoprotein, which mediates cell/cell and cell/matrix interactions, but is also involved in signal transduction from inside as well as outside the cell.

$\alpha_v\beta_3$ integrin is expressed on various cells originating from the mesenchyme and on a variety of cell types in the blood vessel (including endothelial cells, smooth muscle cells, fibroblasts, macrophages and platelets). It is a promiscuous integrin that binds to many different ligands including a number of extracellular matrix proteins such as vitronectin, fibronectin, osteopontin, fibrinogen, and von Willebrand factor, through the interaction with the Arg-Gly-Asp (RGD) motif (31,32). $\alpha_v\beta_3$ integrin is highly expressed in angiogenic or activated endothelial cells but not, or to a much lower extent, in quiescent endothelial cells (33,34).

Radioactive labelled $\alpha_v\beta_3$ antagonists and nuclear medicine imaging techniques may provide a helpful tool to study and quantify angiogenetic processes in plaque development. However, most studies concerning tracer development and evaluation were carried out using tumour models (for review see (35)). The majority of compounds described are based on the α_v-selective cyclic pentapeptide with the amino acid sequence cyclo(-Arg-Gly-Asp-DPhe-Va-) (36). The type of tracer showed comparable affinity and selectivity as the lead structure *in vitro* and receptor specific accumulation in the tumour *in vivo* (37). However, the predominantly hepatobiliary elimination of the tracer demonstrated high activity concentrations in the liver and intestine. Thus, several strategies to improve the pharmacokinetics of radiolabelled peptides have been undertaken. They include conjugation with sugar moieties, hydrophilic amino acids and polyethylene glycol (PEG). The glycosylation approach (38,39), which is based on the introduction of sugar amino acids, resulted in tracers with good pharmacokinetic properties. In a murine tumour model ^{18}F-Galacto-RGD (RGD: one letter code for the amino acids Arg-Gly-Asp, which are essential for binding to the receptor) allowed non-invasive determination of $\alpha_v\beta_3$ expression in the tumour vasculature (Fig 3) (40). Currently, ^{18}F-Galacto-RGD has been evaluated in a first clinical trial and demonstrates rapid predominant renal excretion and high metabolic stability resulting in good tumor/background ratios and thus, high quality imaging (40,41). Moreover, this initial study indicates that tracer accumulation correlates with $\alpha_v\beta_3$ expression on blood vessels in the tumour lesions (Fig 3). While a large set of studies demonstrating that the data concerning imaging tumor-induced angiogenesis can be translated to imaging the pathogenesis of plaque formation has yet to be compiled. Initial findings using $\alpha_v\beta_3$-targeted nanoparticles and MR (42) as well as $\alpha_v\beta_3$-targeted microbubbles and contrast ultra sound imaging (43) indicate that radiolabelled $\alpha_v\beta_3$-targeted tracer may be used to define the burden and evolution of atherosclerosis and the responsiveness of patients to corresponding therapies. Furthermore, a recent study employing a murine hindlimb ischemia model, illustrated that a ^{99m}Tc-labeled peptide (NC100692) targeted to $\alpha_v\beta_3$ integrin selectively localized to endothelial cells in regions of increased angiogenesis and could be used for noninvasive serial "hot spot" imaging of angiogenesis (44).

Lipoproteins

Lipoproteins, particularly low density lipoproteins (LDL), contribute substantially to early lesion formation. These mainly oxidized lipoproteins initiate and sustain the inflammation process and are essential for foam cell generation (5). Strategies to utilize the involvement of lipoproteins in atherogenesis include the use of radiolabelled lipoproteins by themselves, detection of epitopes within the lipoproteins, e.g. by the use of radiolabelled antibodies, or radiolabelled endogeneous receptors for lipoproteins. In initial studies foam cell-rich early

atherosclerotic lesions were detected by radiolabelled autologous LDL molecules in both human and animal studies (45,46). Using a rabbit model of balloon-induced atheroma, Virgolini et al. found a positive correlation between ^{125}I uptake and the extent of foam cell infiltration (46). However, the use of radiolabelled LDL is not without difficulty as significant tracer activity appears within the blood pool even several hours after injection and hampers the detection of lipid-laden plaques. Further investigations have therefore focussed on oxidized LDL (ox-LDL) or various epitopes of ox-LDL because of improved plaque-to-background ratio, the improved uptake into macrophage-rich tissues and the rapid clearance from the blood pool. In addition, in this method there is no need to obtain autologous blood from the patients. Most of these studies have focussed on MDA2, a radiolabeled murine monoclonal antibody, which binds to the malondialdehyde epitope on ox-LDL and there is a significantly higher uptake of ^{125}I-MDA2 in lipid-rich lesions of atherosclerotic mice and rabbits compared to healthy arteries (47,48). After dietary intervention, the same tracer was succesfully used to track changes in macrophage foam cell density. In a clinical trial where ^{99m}Tc ox-LDL was used in humans (49), tomographic scintigraphy of the neck in patients suffering from transient ischemic attacks, revealed accumulation of radiolabelled LDL preparations in the carotid artery affected by atherosclerotic lesions. We have followed a somewhat different approach. Mediating the uptake of LDL - particularly oxLDL - into macrophages scavenger receptors (e.g. CD68, SR-A, CLA-1/SR-BI, CD36, LOX-1, and SR-PSOX) play a key role in atherosclerotic lesion formation (Fig 4 A) (50). Thus, we conjugated ^{124}I to the scavenger receptor CD68 (soluble CD68-Fc) thereby using this molecule as our imaging probe. CD68 has been recently described to be important for foam cell formation, as it binds oxidiced LDL, mediates its uptake (51) and may therefore be a useful tool for the detection of atherosclerotic plaques by the visualization of LDL (Fig 4B). In our study, wildtype or ApoE−/− mice (17 weeks old) were fed with a high cholesterol diet and injected with ~190μCi (7MBq) ^{124}I-CD68-Fc, i.v. After 48h animals were sacrificed and evaluated by *ex vivo* autoradiography (Fig 4C). In addition, sudan red staining was performed to compare radioactivity with plaque formation (Fig 4C). We found a good correlation of signal with the extent of the lesion. While preliminary, our data suggests that CD68 is a potent molecular marker for the detection of atherosclerosis. These findings have to be verified by further profound investigations.

Proteolysis

Through degradation of the extracellular matrix, proteases contribute to the progression and complications of atherosclerotic lesions. At later stages of atherosclerosis, a lesion core is covered by a fibrous cap, which consists mainly of smooth muscle cells and extracellular matrix and separates the lipid-rich core from the blood stream (5).

Interstitial collagen molecules, adjacent to others like fibrin, confer most of the tensile strength on the fibrous cap, and several tightly regulated processes determine the levels of collagen required for stability of this structure (6). Certain pro-inflammatory cytokines, such as IFN-γ, can inhibit collagen production by smooth muscle cells, the principle source of this extracellular matrix macromolecule in the arterial wall. Hence, the degree of plaque vulnerability is influenced by factors such as overall size, core size, cap thickness, cap inflammation, and cap fatigue.

Enhanced turnover of the extracellular matrix is known to be the reason for destabilization of the vulnerable fibrous cap. The cells mainly responsible for this process are monocytes, which differentiate to macrophages within the atherosclerotic lesion. The destabilization is mediated by matrix-metallo-proteinases (MMPs), which can be released by activated macrophages, endothelial and other vascular cells. Known mediators of such inflammatory processes are TNF-α and CD40L (52,53).

Strategies to image proteolytic activity included the use of radiolabelled MMP inhibitors, substrates of MMPs, MMP inhibitors and cathepsins.

Schäfers and coworkers used a broad-spectrum MMP inhibitor conjugated to ^{123}I to develop the radioligand ^{123}II-HO-CGS 27023A for *in vivo* imaging of MMP activity (10). 4 weeks after induction of arterial injury in the carotid artery of ApoE−/− mice fed with a cholesterol-rich diet, the tracer was injected retroorbitally and uptake was measured. During the first 2 hours, a steadily increasing uptake could be detected. Specificity was verified by predisposing cells with unlabeled CGS 27023A. A very elegant way to make use of enhanced MMP activity in tissues was recently published by Chen *et al*., who used a novel long-circulating, quenched near-infrared fluorescent (NIRF) probe, that is activated by MMP2 and MMP9, the essential proteases for the pathophysiology of atherosclerotic lesions. (54) *In vitro*, the fluorescence signal changes can be detected after activation with MMP2 or MMP9 at the specific wavelengths of the attached fluorochrome Cy5.5 by use of a fluorescence plate reader. For *in vivo* experiments, the authors chose a mouse myocardial infarction model to monitor MMP-activity within the infarcted region. NIRF imaging of MMP activity increased within 1 to 2 weeks after arterial ligation, a result that was confirmed by parallel *in vitro* methods including zymography and RT-PCR analysis of MMP expression.

Choudhary and colleagues used carotid endarteryectomy specimen and multicontrast MRI to generate 3D reconstructions and evaluate spatial distribution of MMPs and its inhibitors (TIMPs) in carotid atherosclerotic lesions. They found that their distribution is highly heterogeneous and reflects lesion location, size, and composition (55). Notably, the greater abundance of MMP-9 in the plaque area suggests that it is a major MMP mediating remodeling in this area. In grossly normal areas, the level of total MMPs is lower and dominated by MMP-2. The authors concluded that remodeling of atheroma and normal arterial wall are mediated by different MMPs (55). The results are consistent with previous observations that MMP-9, but not MMP-2, was necessary for organization of collagen by SMCs (56).

In addition to MMPs, the cathepsin family of proteases was tested for use in plaque imaging studies. Chen *et al*. optically imaged cathepsin B activity in experimental atherosclerosis *in vivo* using a NIRF approach (57). Similarly, Jaffer *et al*. were able to visualize atherosclerotic plaques very recently in both mice and humans using a NIRF imaging agent consisting of the Cathepsin K peptide substrate (GHPGGPQGKC-NH_2) linked to an activable fluorogenic polymer (58). Taken together, matrix-metalloproteinases represent a very promising target for non-invasive imaging, as they are essential for different pathophysiologic processes including tumor progression, inflammation and atherogenesis.

Apoptosis

Apoptosis has been shown to be one of the characteristics of atherosclerotic plaques (59). Animal studies of hypercholesterolemia showed both proliferation and cell death of smooth muscle cells in early intimal lesions (60,61). Mentionable studies so far focussed on annexin V using this molecule in a radiolabelled form. During the process of apoptosis, phosphatidylserine, a phospholipid normally residing on the inner cell membrane of viable cells, is externalized and thus available to affinity ligands such as annexin V.

In a model of porcine coronary atherosclerosis, apoptosis of cells in the vascular wall of coronary arteries could be detected by SPECT using ^{99m}Tc-annexin-V (62). Thirteen out of twenty two injured coronary vessels of animals receiving a high fat diet showed focal ^{99m}Tc-annexin-V uptake. Another group made use of the same marker to detect experimental atheroma in the aorta of balloon-injured rabbits *in vivo* (63). In this study, histologically verified macrophage apoptosis showed a positive correlation with tracer uptake. Several clinical studies using annexin-V as a radionuclide tracer have been carried out so far. In a study with 18 cardiac

allograft recipients, 5 patients had positive myocardial uptake of annexin-V (13 negative) (64). As these five patients revealed at least moderate transplant rejection and caspase-3 staining in the biopsy specimen, the authors proposed the clinical feasibility of annexin-V imaging for noninvasive detection of transplant rejection. Another group also tried to visualize myocardial infarction by ^{99m}Tc-annexin-V uptake (65) and in this trial, six out of seven patients showed increased uptake of the tracer in early and late SPECT images. Lastly, a recent manuscript further underlined the hypothesis that atherosclerotic lesions induced by a high cholesterol diet in apoE−/− mice can be detected by apoptotic markers (66). Atherosclerotic plaques in the aorta could be visualized by ^{99m}Annexin A5 using microSPECT and the quantitative uptake of this tracer correlated with histological plaque extent and macrophage content (66). Despite these very promising results, further experimental and clinical studies have to be carried out to further establish the efficacy of employing nuclear imaging of programmed cell death for noninvasive detection of the vulnerable atherosclerotic plaque.

Thrombogenicity and cell recruitment

The majority of myocardial infarctions are caused by development of a thrombus in coronary vessels at site of vascular lesions (erosion, plaque rupture) (Fig 5A). Therefore, thrombogenicity is a central feature of plaque vulnerability. A prerequesite for the formation of a thrombus is the exposure of subendothelial matrix components resulting in enhanced cell recruitment. Plaque imaging approaches derived from this principle include the use of cells participating in thrombus formation, the detection of soluble coagulation factors or the visualization of exposed subendothelial matrix.

Early approaches used radionuclide labelled platelets to detect vulnerable plaques. As the coagulation cascade results in the development of a fibrin rich thrombus, Cerqueira and colleagues used a radiolabeled monoclonal antibody fragment ^{99m}Tc-T2G1s Fab, which is specific for fibrin, in a canine carotid and femoral artery injury model. The tracer was shown to bind twice as strong to trauma induced thrombotic arteries compared to sham operated animals (67). Another group also demonstrated the feasibility of *in vivo* detection of acute and subacute thrombosis using a fibrin-binding contrast agent in an animal model of atherosclerosis by a magnetic resonance imaging approach (68). A plaque imaging study was performed using a F(ab')2 monoclonal antibody (TRF1) against the human fragment D dimer of cross-linked fibrin for atherosclerotic plaques. Atherosclerotic segments of carotid and femoral arteries of 6 patients and 5 control segments of atherosclerosis-free internal mammary arteries were drawn from 11 male patients undergoing bypass surgery. (69) The ^{125}I-TRF1 antibody was used to distinguish atherosclerotic fragments, fatty streaks and normal endothelium. The significantly higher binding of TRF to atherosclerotic plaques compared to normal vessels was specific, as a control antibody showed no binding (69).

Within vulnerable atherosclerotic lesions, extracellular matrix proteins like collagen or fibronectin are exposed that are highly thrombogenic to circulating platelets and coagulation but also represent potential targets for imaging techniques. Matter *et al* used an ^{125}I-labeled antibody L19 which targets the extradomain B of fibronectin and injected atherosclerotic ApoE −/− mice (70). By this approach atherosclerotic plaques could be detected after three days with signal to noise ratios of 105:1 at 3 days(70). Furthermore, increased expression of extradomain-B domain in human atherosclerotic plaques can be detected by immunohistochemical studies and our group has followed a similar approach by visualizing collagen exposed to blood flow.

Detection of vulnerable plaques by radiolabeled platelet GPVI

We made use of the major platelet collagen receptor Glycoprotein VI (GPVI), which plays a critical role in the process of thrombosis at sites of atherosclerotic lesions. As the main extracellular matrix protein of arteries, fibrillar collagen acts as a strong activator of platelets

and supports platelet-dependent thrombus formation (71,72). Recently, platelet GPVI has been identified as the major platelet collagen receptor *in vivo* (73). GPVI is a 60–65 kDA type I transmembrane glycoprotein, which belongs to the immunoglobulin superfamily (71). The soluble dimeric form of human GPVI conjugated to an Fc-fragment, which was radioiodinated (Fig 5B), was capable of detecting lesions of injured carotid arteries in mice through *ex vivo* and *in vivo* imaging (11). In one study, 5 min after induction of injury, ^{124}I GPVI (or eqivalent amounts of the radioiodinated Fc-fragment as a negative control) was injected intravenously. An experimental mouse model of vascular injury was used and wire-induced injury of the carotid artery was performed as described previously (74). In this manner, vascular lesions could be clearly detected with high resolution using a dedicated small-animal PET scanner (MicroPET Focus 120; Siemens, Knoxville, TN, USA) (Fig 4C) and images were matched with CT data (Fig 5C). The extent of *ex vivo* autoradiography signal correlated with lesion formation as verified by lesion extent in the explanted artery specimen (Fig 5D). These experimental data suggest that the soluble form of the platelet collagen receptor GPVI allows detection of thrombogenic and thus vulnerable arterial lesions.

Taken together, the thrombogenicity of atherosclerotic plaques is one of the most promising approaches to detect vulnerable plaques.

Clinical perspective

The strength of molecular imaging is based on the fact that most diseases have an underlying biological basis that is not visualized by traditional imaging methods. Furthermore, it will most likely contribute to a personalized medicine by helping to tailor drug selection to an individual's proteome and genome (75). Imaging of important molecular targets could transform clinical management for diagnosis, risk stratification, selection and efficacy assessment of molecule-based therapeutics. If methods are optimized, we may be able to decide which patients harbor high-risk atherosclerotic plaques that will ultimately cause myocardial infarction or stroke. Other applications include determining which post–myocardial infarction patients will develop pathological ventricular remodeling and rapid progression to heart failure. Direct visualization of the underlying biology in the diseased tissue may identify patients at high risk for cardiovascular complications, allowing the clinician to tailor disease management on the basis of risk. Molecular imaging may not only identify patients at high-risk for cardiovascular events (death, myocardial infarction, stroke) not identified by routine clinical evaluation (e.g., history, physical exam, electrocardiogram, lipid profile, C-reactive protein, exercise treadmill testing), but also the characterization of lesion vulnerability in high-risk areas of the coronary vasculature (e.g., the proximal third of each of the coronary arteries (76)) may be possible. Once the lesion has been determined to be of particularly high risk, novel local therapies such as intracoronary drug-eluting stents or local drug delivery with suitable drug-delivery balloon catheters could be justified. At present, the selection of many target specific therapeutics depends on population-based studies or randomized clinical trials. These approaches, however, do not routinely assess the biological variability of the disease process in individual patients. Thus, molecular plaque imaging will help to select individualized treatment strategies based on the molecular profile of vulnerable plaques identified in particular patients. In keeping with this, several promising atherosclerosis-targeted imaging agents have already undergone testing in the clinic or are on the clinical horizon (Figure 6) (reviewed in (75)).

CONCLUSIONS

Over the past years, clinical data and observations have emphasized the need for a more profound characterisation of atherosclerotic plaques. It is essential to acquire information beyond the resulting degree of stenosis detected by angiography. Epidemiologic studies have shown that a considerable amount of patients with sudden cardiac events have no alarming

symptoms prior to a serious event (77). Furthermore, acute coronary syndromes often result from plaque rupture at sites with no or only moderate luminal narrowing detected by angiography (78,79). Molecular imaging of atherosclerotic plaques offers new strategies to detect vulnerable atherosclerotic plaques that are prone to thrombus formation. Increasing our knowledge about the molecular biology of plaque vulnerability and identification of new mediators will prove most promising and challenging and will propel the field of plaque imaging to the forefront of cardiology.

ABBREVIATION LIST

ECM, Extracellular matrix; FDG, fluorodeoxyglucose; FCH, fluorocholine; GPVI, Glycoprotein VI; LDL, low density lipoprotein; MCP-1, Monocyte chemoattractant protein-1; MDA2, malondialdehyde epitope on ox-LDL; MMPs, Matrix-Metalloproteinases; Ox-LDL, oxidized low density lipoprotein; RGD, protein sequence "Arginine-Glycine-Aspartic acid".

REFERENCES

1. Naghavi M, Libby P, Falk E, et al. From vulnerable plaque to vulnerable patient: a call for new definitions and risk assessment strategies: Part II. Circulation 2003;108:1772–1778. [PubMed: 14557340]
2. Nissen SE, Yock P. Intravascular ultrasound: novel pathophysiological insights and current clinical applications. Circulation 2001;103:604–616. [PubMed: 11157729]
3. Schroeder S, Kopp AF, Baumbach A, et al. Noninvasive detection and evaluation of atherosclerotic coronary plaques with multislice computed tomography. J Am Coll Cardiol 2001;37:1430–1435. [PubMed: 11300457]
4. Schmermund A, Erbel R. Unstable coronary plaque and its relation to coronary calcium. Circulation 2001;104:1682–1687. [PubMed: 11581149]
5. Ross R. Atherosclerosis--an inflammatory disease. N Engl J Med 1999;340:115–126. [PubMed: 9887164]
6. Libby P. Inflammation in atherosclerosis. Nature 2002;420:868–874. [PubMed: 12490960]
7. Ginsberg HN, Goldsmith SJ, Vallabhajosula S. Noninvasive imaging of 99mtechnetium-labeled low density lipoprotein uptake by tendon xanthomas in hypercholesterolemic patients. Arteriosclerosis 1990;10:256–262. [PubMed: 2317159]
8. Mettinger KL, Larsson S, Ericson K, Casseborn S. Detection of atherosclerotic plaques in carotid arteries by the use of 123I-fibrinogen. Lancet 1978;1:242–244. [PubMed: 74666]
9. Ohtsuki K, Hayase M, Akashi K, Kopiwoda S, Strauss HW. Detection of monocyte chemoattractant protein-1 receptor expression in experimental atherosclerotic lesions: an autoradiographic study. Circulation 2001;104:203–208. [PubMed: 11447087]
10. Schafers M, Riemann B, Kopka K, et al. Scintigraphic imaging of matrix metalloproteinase activity in the arterial wall in vivo. Circulation 2004;109:2554–2559. [PubMed: 15123523]
11. Gawaz M, Konrad I, Hauser AI, et al. Non-invasive imaging of glycoprotein VI binding to injured arterial lesions. Thromb Haemost 2005;93:910–913. [PubMed: 15886808]
12. Davis HH, Heaton WA, Siegel BA, et al. Scintigraphic detection of atherosclerotic lesions and venous thrombi in man by indium-111-labelled autologous platelets. Lancet 1978;1:1185–1187. [PubMed: 77949]
13. Caussin C, Ohanessian A, Ghostine S, et al. Characterization of vulnerable nonstenotic plaque with 16-slice computed tomography compared with intravascular ultrasound. Am J Cardiol 2004;94:99–104. [PubMed: 15219516]
14. Nieman K, van der LA, Pattynama PM, de Feyter PJ. Noninvasive visualization of atherosclerotic plaque with electron beam and multislice spiral computed tomography. J Interv Cardiol 2003;16:123–128. [PubMed: 12768915]
15. Toussaint JF, Southern JF, Fuster V, Kantor HL. T2-weighted contrast for NMR characterization of human atherosclerosis. Arterioscler Thromb Vasc Biol 1995;15:1533–1542. [PubMed: 7583524]

16. Kooi ME, Cappendijk VC, Cleutjens KB, et al. Accumulation of ultrasmall superparamagnetic particles of iron oxide in human atherosclerotic plaques can be detected by in vivo magnetic resonance imaging. Circulation 2003;107:2453–2458. [PubMed: 12719280]
17. Virgolini I, Muller C, Fitscha P, Chiba P, Sinzinger H. Radiolabelling autologous monocytes with 111-indium-oxine for reinjection in patients with atherosclerosis. Prog Clin Biol Res 1990;355:271–280. [PubMed: 2126377]
18. Rudd JH, Warburton EA, Fryer TD, et al. Imaging atherosclerotic plaque inflammation with [18F]-fluorodeoxyglucose positron emission tomography. Circulation 2002;105:2708–2711. [PubMed: 12057982]
19. Haeffner EW. Studies on choline permeation through the plasma membrane and its incorporation into phosphatidyl choline of Ehrlich-Lettre-ascites tumor cells in vitro. Eur J Biochem 1975;51:219–228. [PubMed: 1168133]
20. Boggs KP, Rock CO, Jackowski S. Lysophosphatidylcholine and 1-O-octadecyl-2-O-methyl-rac-glycero-3-phosphocholine inhibit the CDP-choline pathway of phosphatidylcholine synthesis at the CTP:phosphocholine cytidylyltransferase step. J Biol Chem 1995;270:7757–7764. [PubMed: 7706325]
21. Ramirez de MA, Gutierrez R, Ramos MA, et al. Increased choline kinase activity in human breast carcinomas: clinical evidence for a potential novel antitumor strategy. Oncogene 2002;21:4317–4322. [PubMed: 12082619]
22. Matter CM, Wyss MT, Meier P, et al. 18F-choline images murine atherosclerotic plaques ex vivo. Arterioscler Thromb Vasc Biol 2006;26:584–589. [PubMed: 16357314]
23. Wyss MT, Weber B, Honer M, et al. 18F-choline in experimental soft tissue infection assessed with autoradiography and high-resolution PET. Eur J Nucl Med Mol Imaging 2004;31:312–316. [PubMed: 14628099]
24. Henriksen G, Herz M, Hauser A, Schwaiger M, Wester HJ. Synthesis and preclinical evaluation of the choline transport tracer deshydroxy-[18F]fluorocholine ([18F]dOC). Nucl Med Biol 2004;31:851–858. [PubMed: 15464386]
25. Gawaz M, Neumann FJ, Dickfeld T, et al. Activated platelets induce monocyte chemotactic protein-1 secretion and surface expression of intercellular adhesion molecule-1 on endothelial cells. Circulation 1998;98:1164–1171. [PubMed: 9743506]
26. Charo IF, Taubman MB. Chemokines in the pathogenesis of vascular disease. Circ Res 2004;95:858–866. [PubMed: 15514167]
27. Bidzhekov K, Zernecke A, Weber C. MCP-1 induces a novel transcription factor with proapoptotic activity. Circ Res 2006;98:1107–1109. [PubMed: 16690887]
28. Nahrendorf M, Jaffer FA, Kelly KA, et al. Noninvasive vascular cell adhesion molecule-1 imaging identifies inflammatory activation of cells in atherosclerosis. Circulation 2006;114:1504–1511. [PubMed: 17000904]
29. Kelly KA, Allport JR, Tsourkas A, Shinde-Patil VR, Josephson L, Weissleder R. Detection of vascular adhesion molecule-1 expression using a novel multimodal nanoparticle. Circ Res 2005;96:327–336. [PubMed: 15653572]
30. Moreno PR, Purushothaman KR, Fuster V, et al. Plaque neovascularization is increased in ruptured atherosclerotic lesions of human aorta: implications for plaque vulnerability. Circulation 2004;110:2032–2038. [PubMed: 15451780]
31. Hynes RO. A reevaluation of integrins as regulators of angiogenesis. Nat Med 2002;8:918–921. [PubMed: 12205444]
32. Hynes RO. Integrins: bidirectional, allosteric signaling machines. Cell 2002;110:673–687. [PubMed: 12297042]
33. Sipkins DA, Cheresh DA, Kazemi MR, Nevin LM, Bednarski MD, Li KC. Detection of tumor angiogenesis in vivo by alphaVbeta3-targeted magnetic resonance imaging. Nat Med 1998;4:623–626. [PubMed: 9585240]
34. Brooks PC, Clark RA, Cheresh DA. Requirement of vascular integrin alpha v beta 3 for angiogenesis. Science 1994;264:569–571. [PubMed: 7512751]
35. Haubner R. Alphavbeta3-integrin imaging: a new approach to characterise angiogenesis? Eur J Nucl Med Mol Imaging 2006;33:54–63. [PubMed: 16791598]54–63.

36. Aumailley M, Gurrath M, Muller G, Calvete J, Timpl R, Kessler H. Arg-Gly-Asp constrained within cyclic pentapeptides. Strong and selective inhibitors of cell adhesion to vitronectin and laminin fragment P1. FEBS Lett 1991;291:50–54. [PubMed: 1718779]
37. Haubner R, Wester HJ, Reuning U, et al. Radiolabeled alpha(v)beta3 integrin antagonists: a new class of tracers for tumor targeting. J Nucl Med 1999;40:1061–1071. [PubMed: 10452325]
38. Haubner R, Wester HJ, Weber WA, et al. Noninvasive imaging of alpha(v)beta3 integrin expression using 18F-labeled RGD-containing glycopeptide and positron emission tomography. Cancer Res 2001;61:1781–1785. [PubMed: 11280722]
39. Haubner R, Wester HJ, Burkhart F, et al. Glycosylated RGD-containing peptides: tracer for tumor targeting and angiogenesis imaging with improved biokinetics. J Nucl Med 2001;42:326–336. [PubMed: 11216533]
40. Haubner R, Weber WA, Beer AJ, et al. Noninvasive visualization of the activated alphavbeta3 integrin in cancer patients by positron emission tomography and [18F]Galacto-RGD. PLoS Med 2005;2:e70. [PubMed: 15783258]
41. Beer AJ, Haubner R, Goebel M, et al. Biodistribution and pharmacokinetics of the alphavbeta3-selective tracer 18F-galacto-RGD in cancer patients. J Nucl Med 2005;46:1333–1341. [PubMed: 16085591]
42. Winter PM, Morawski AM, Caruthers SD, et al. Molecular imaging of angiogenesis in early-stage atherosclerosis with alpha(v)beta3-integrin-targeted nanoparticles. Circulation 2003;108:2270–2274. [PubMed: 14557370]
43. Leong-Poi H, Christiansen J, Heppner P, et al. Assessment of endogenous and therapeutic arteriogenesis by contrast ultrasound molecular imaging of integrin expression. Circulation 2005;111:3248–3254. [PubMed: 15956135]
44. Hua J, Dobrucki LW, Sadeghi MM, et al. Noninvasive imaging of angiogenesis with a 99mTc-labeled peptide targeted at alphavbeta3 integrin after murine hindlimb ischemia. Circulation 2005;111:3255–3260. [PubMed: 15956134]
45. Virgolini I, Rauscha F, Lupattelli G, et al. Autologous low-density lipoprotein labelling allows characterization of human atherosclerotic lesions in vivo as to presence of foam cells and endothelial coverage. Eur J Nucl Med 1991;18:948–951. [PubMed: 1778204]
46. Virgolini I, Angelberger P, O'Grady J, Sinzinger H. Low density lipoprotein labelling characterizes experimentally induced atherosclerotic lesions in rabbits in vivo as to presence of foam cells and endothelial coverage. Eur J Nucl Med 1991;18:944–947. [PubMed: 1778203]
47. Tsimikas S, Shortal BP, Witztum JL, Palinski W. In vivo uptake of radiolabeled MDA2, an oxidation-specific monoclonal antibody, provides an accurate measure of atherosclerotic lesions rich in oxidized LDL and is highly sensitive to their regression. Arterioscler Thromb Vasc Biol 2000;20:689–697. [PubMed: 10712392]
48. Tsimikas S, Palinski W, Witztum JL. Circulating autoantibodies to oxidized LDL correlate with arterial accumulation and depletion of oxidized LDL in LDL receptor-deficient mice. Arterioscler Thromb Vasc Biol 2001;21:95–100. [PubMed: 11145939]
49. Iuliano L, Signore A, Vallabajosula S, et al. Preparation and biodistribution of 99m technetium labelled oxidized LDL in man. Atherosclerosis 1996;126:131–141. [PubMed: 8879441]
50. Shashkin P, Dragulev B, Ley K. Macrophage differentiation to foam cells. Curr Pharm Des 2005;11:3061–3072. [PubMed: 16178764]
51. Daub K, Langer H, Seizer P, et al. Platelets induce differentiation of human CD34+ progenitor cells into foam cells and endothelial cells. FASEB J 2006;20:2559–2561. [PubMed: 17077283]
52. Henn V, Slupsky JR, Grafe M, et al. CD40 ligand on activated platelets triggers an inflammatory reaction of endothelial cells. Nature 1998;391:591–594. [PubMed: 9468137]
53. May AE, Kalsch T, Massberg S, Herouy Y, Schmidt R, Gawaz M. Engagement of glycoprotein IIb/IIIa (alpha(IIb)beta3) on platelets upregulates CD40L and triggers CD40L-dependent matrix degradation by endothelial cells. Circulation 2002;106:2111–2117. [PubMed: 12379582]
54. Chen J, Tung CH, Allport JR, Chen S, Weissleder R, Huang PL. Near-infrared fluorescent imaging of matrix metalloproteinase activity after myocardial infarction. Circulation 2005;111:1800–1805. [PubMed: 15809374]

55. Choudhary S, Higgins CL, Chen IY, et al. Quantitation and localization of matrix metalloproteinases and their inhibitors in human carotid endarterectomy tissues. Arterioscler Thromb Vasc Biol 2006;26:2351–2358. [PubMed: 16888239]
56. Johnson C, Galis ZS. Matrix metalloproteinase-2 and -9 differentially regulate smooth muscle cell migration and cell-mediated collagen organization. Arterioscler Thromb Vasc Biol 2004;24:54–60. [PubMed: 14551157]
57. Chen J, Tung CH, Mahmood U, et al. In vivo imaging of proteolytic activity in atherosclerosis. Circulation 2002;105:2766–2771. [PubMed: 12057992]
58. Jaffer FA, Kim DE, Quinti L, et al. Optical visualization of cathepsin K activity in atherosclerosis with a novel, protease-activatable fluorescence sensor. Circulation 2007;115:2292–2298. [PubMed: 17420353]
59. Geng YJ, Libby P. Evidence for apoptosis in advanced human atheroma. Colocalization with interleukin-1 beta-converting enzyme. Am J Pathol 1995;147:251–266. [PubMed: 7639325]
60. Thomas WA, Scott RF, Florentin RA, Reiner JM, Lee KT. Population dynamics of arterial cells during atherogenesis. XI. Slowdown in multiplication and death rates of lesion smooth muscle cells in swine during the period 105–165 days after balloon endothelial cell denudation followed by a hyperlipidemic diet. Exp Mol Pathol 1981;35:153–162. [PubMed: 7286156]
61. Thomas WA, Kim DN, Lee KT, Reiner JM, Schmee J. Population dynamics of arterial cells during atherogenesis. XIII. Mitogenic and cytotoxic effects of a hyperlipidemic (HL) diet on cells in advanced lesions in the abdominal aortas of swine fed an HL diet for 270–345 days. Exp Mol Pathol 1983;39:257–270. [PubMed: 6641917]
62. Johnson LL, Schofield L, Donahay T, Narula N, Narula J. 99mTc-annexin V imaging for in vivo detection of atherosclerotic lesions in porcine coronary arteries. J Nucl Med 2005;46:1186–1193. [PubMed: 16000288]
63. Kolodgie FD, Petrov A, Virmani R, et al. Targeting of apoptotic macrophages and experimental atheroma with radiolabeled annexin V: a technique with potential for noninvasive imaging of vulnerable plaque. Circulation 2003;108:3134–3139. [PubMed: 14676140]
64. Narula J, Acio ER, Narula N, et al. Annexin-V imaging for noninvasive detection of cardiac allograft rejection. Nat Med 2001;7:1347–1352. [PubMed: 11726976]
65. Hofstra L, Liem IH, Dumont EA, et al. Visualisation of cell death in vivo in patients with acute myocardial infarction. Lancet 2000;356:209–212. [PubMed: 10963199]
66. Isobe S, Tsimikas S, Zhou J, et al. Noninvasive imaging of atherosclerotic lesions in apolipoprotein E-deficient and low-density-lipoprotein receptor-deficient mice with annexin A5. J Nucl Med 2006;47:1497–1505. [PubMed: 16954559]
67. Cerqueira MD, Stratton JR, Vracko R, Schaible TF, Ritchie JL. Noninvasive arterial thrombus imaging with 99mTc monoclonal antifibrin antibody. Circulation 1992;85:298–304. [PubMed: 1728460]
68. Botnar RM, Perez AS, Witte S, et al. In vivo molecular imaging of acute and subacute thrombosis using a fibrin-binding magnetic resonance imaging contrast agent. Circulation 2004;109:2023–2029. [PubMed: 15066940]
69. Greco C, Di Loreto M, Ciavolella M, et al. Immunodetection of human atherosclerotic plaque with 125I-labeled monoclonal antifibrin antibodies. Atherosclerosis 1993;100:133–139. [PubMed: 8357347]
70. Matter CM, Schuler PK, Alessi P, et al. Molecular imaging of atherosclerotic plaques using a human antibody against the extra-domain B of fibronectin. Circ Res 2004;95:1225–1233. [PubMed: 15539632]
71. Clemetson KJ, Clemetson JM. Platelet collagen receptors. Thromb Haemost 2001;86:189–197. [PubMed: 11487007]
72. Nieswandt B, Watson SP. Platelet-collagen interaction: is GPVI the central receptor? Blood 2003;102:449–461. [PubMed: 12649139]
73. Massberg S, Gawaz M, Gruner S, et al. A crucial role of glycoprotein VI for platelet recruitment to the injured arterial wall in vivo. J Exp Med 2003;197:41–49. [PubMed: 12515812]
74. Moers A, Nieswandt B, Massberg S, et al. G13 is an essential mediator of platelet activation in hemostasis and thrombosis. Nat Med 2003;9:1418–1422. [PubMed: 14528298]

75. Jaffer FA, Libby P, Weissleder R. Molecular and cellular imaging of atherosclerosis: emerging applications. J Am Coll Cardiol 2006;47:1328–1338. [PubMed: 16580517]
76. Wang JC, Normand SL, Mauri L, Kuntz RE. Coronary artery spatial distribution of acute myocardial infarction occlusions. Circulation 2004;110:278–284. [PubMed: 15249505]
77. Myerburg RJ, Interian A Jr, Mitrani RM, Kessler KM, Castellanos A. Frequency of sudden cardiac death and profiles of risk. Am J Cardiol 1997;80:10F–19F.
78. Fuster V, Badimon L, Badimon JJ, Chesebro JH. The pathogenesis of coronary artery disease and the acute coronary syndromes (1). N Engl J Med 1992;326:242–250. [PubMed: 1727977]
79. Farb A, Burke AP, Tang AL, et al. Coronary plaque erosion without rupture into a lipid core. A frequent cause of coronary thrombosis in sudden coronary death. Circulation 1996;93:1354–1363. [PubMed: 8641024]
80. Lees AM, Lees RS, Schoen FJ, et al. Imaging human atherosclerosis with 9mTc-labeled low density lipoproteins. Arteriosclerosis 1988;8:461–470. [PubMed: 3190553]
81. Tsimikas S, Palinski W, Halpern SE, Yeung DW, Curtiss LK, Witztum JL. Radiolabeled MDA2, an oxidation-specific, monoclonal antibody, identifies native atherosclerotic lesions in vivo. J Nucl Cardiol 1999;6:41–53. [PubMed: 10070840]
82. Shaw PX, Horkko S, Tsimikas S, et al. Human-derived anti-oxidized LDL autoantibody blocks uptake of oxidized LDL by macrophages and localizes to atherosclerotic lesions in vivo. Arterioscler Thromb Vasc Biol 2001;21:1333–1339. [PubMed: 11498462]
83. Hardoff R, Braegelmann F, Zanzonico P, et al. External imaging of atherosclerosis in rabbits using an 123I-labeled synthetic peptide fragment. J Clin Pharmacol 1993;33:1039–1047. [PubMed: 8300886]
84. Lu P, Zanzonico P, Lister-James J, et al. Biodistribution and Autoradiographic Localization of I-125--Labeled Synthetic Peptide in Aortic Atherosclerosis in Cholesterol-Fed Rabbits. Am J Ther 1996;3:673–680. [PubMed: 11862222]
85. Lee KH, Jung KH, Song SH, et al. Radiolabeled RGD uptake and alphav integrin expression is enhanced in ischemic murine hindlimbs. J Nucl Med 2005;46:472–478. [PubMed: 15750161]
86. Lederman RJ, Raylman RR, Fisher SJ, et al. Detection of atherosclerosis using a novel positron-sensitive probe and 18-fluorodeoxyglucose (FDG). Nucl Med Commun 2001;22:747–753. [PubMed: 11453046]
87. Ben Haim S, Kupzov E, Tamir A, Israel O. Evaluation of 18F-FDG uptake and arterial wall calcifications using 18F-FDG PET/CT. J Nucl Med 2004;45:1816–1821. [PubMed: 15534049]
88. Kietselaer BL, Reutelingsperger CP, Heidendal GA, et al. Noninvasive detection of plaque instability with use of radiolabeled annexin A5 in patients with carotid-artery atherosclerosis. N Engl J Med 2004;350:1472–1473. [PubMed: 15070807]
89. Minar E, Ehringer H, Dudczak R, et al. Indium-111-labeled platelet scintigraphy in carotid atherosclerosis. Stroke 1989;20:27–33. [PubMed: 2911831]
90. Moriwaki H, Matsumoto M, Handa N, et al. Functional and anatomic evaluation of carotid atherothrombosis. A combined study of indium 111 platelet scintigraphy and B-mode ultrasonography. Arterioscler Thromb Vasc Biol 1995;15:2234–2240. [PubMed: 7489248]
91. Mitchel J, Waters D, Lai T, et al. Identification of coronary thrombus with a IIb/IIIa platelet inhibitor radiopharmaceutical, technetium-99m DMP-444: A canine model. Circulation 2000;101:1643–1646. [PubMed: 10758044]

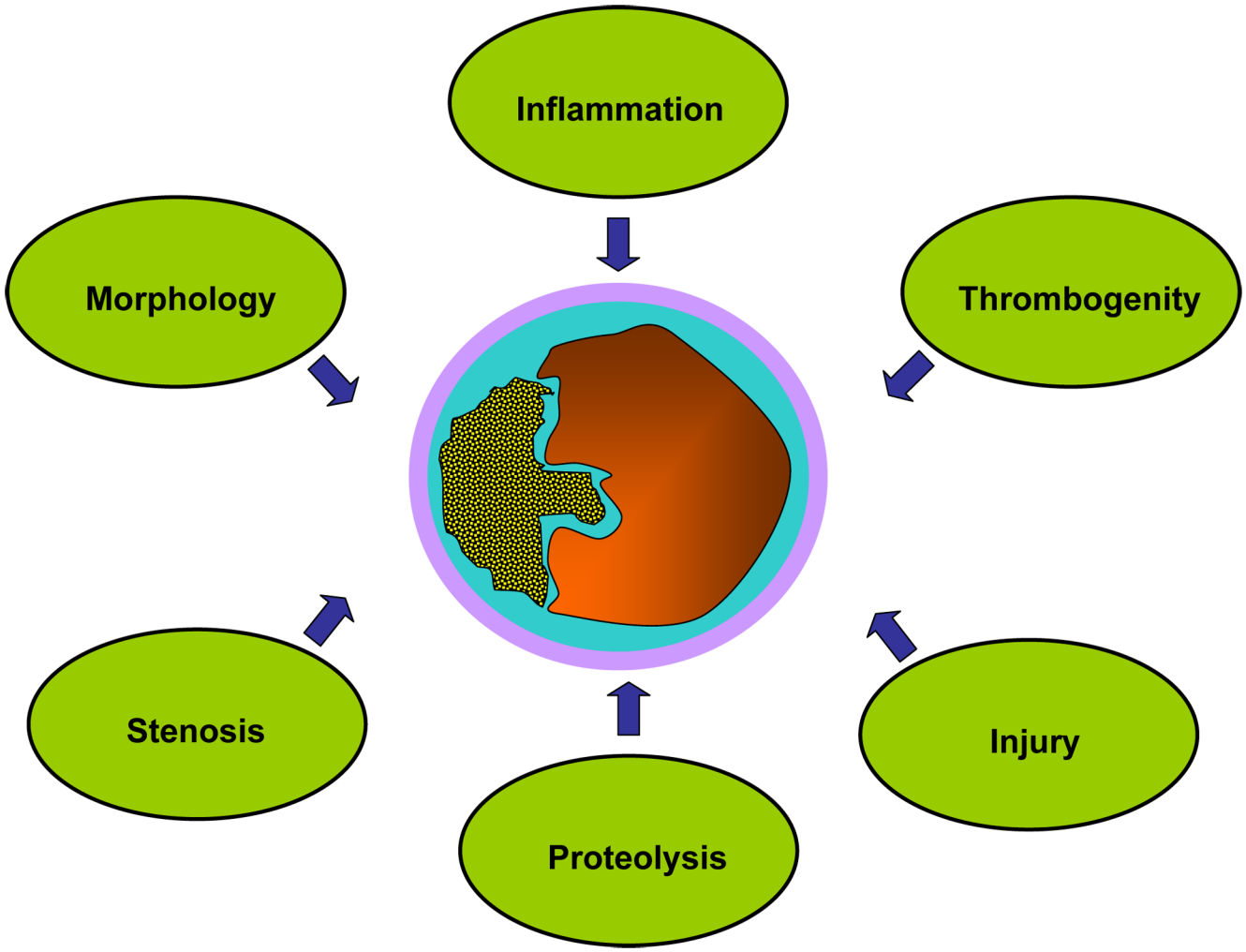

Fig 1. Major criteria defining the "vulnerable plaque"
Vulnerable atherosclerotic plaques are characterized by distinct attributes regarding morphology, stenosis, inflammation, thrombogenity, injury and enhanced proteinase activity.

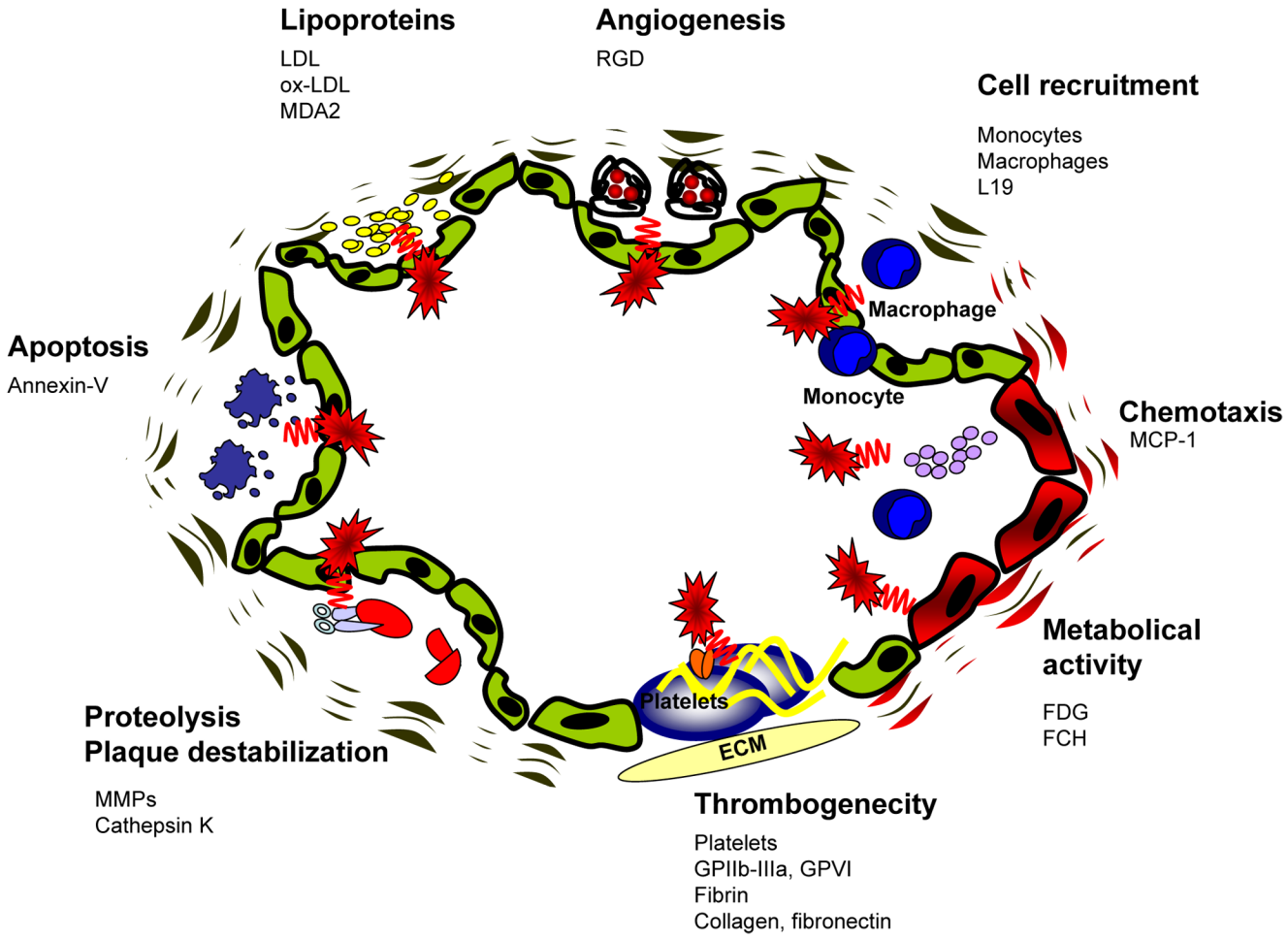

Fig 2. Molecular principles to detect atherosclerotic plaques

Based upon the increasing molecular knowledge regarding atherogenesis, different principles have been successfully used to image atherosclerotic plaques. One major complex is the molecular imaging of inflammation, which includes enhanced metabolic activity, chemotaxis, cell recruitment and lipoprotein accumulation. Furthermore mediators of angiogenesis, apoptosis and matrix metalloproteinase activity have been successfully applied. Another promising approach to detect vulnerable atherosclerotic is the visualization of plaque thrombogenicity, including thrombosis and exposure of thrombogenic subendothelial matrix proteins. ECM = Extracellular matrix. GPIIbIIIa = Glycoprotein IIbIIIa. GPVI = Glycoprotein VI. FDG = fluorodeoxyglucose. MCP-1 = Monocyte chemoattractant protein-1. RGD = protein sequence "Arginine-Glycine- Aspartic acid". FCH = fluorocholine. LDL = low density lipoprotein. Ox-LDL = oxidized low density lipoprotein. MDA2 = malondialdehyde epitope on ox-LDL. MMPs = Matrix-Metalloproteinases. L19 = antibody against the extra-domain B of fibronectin.

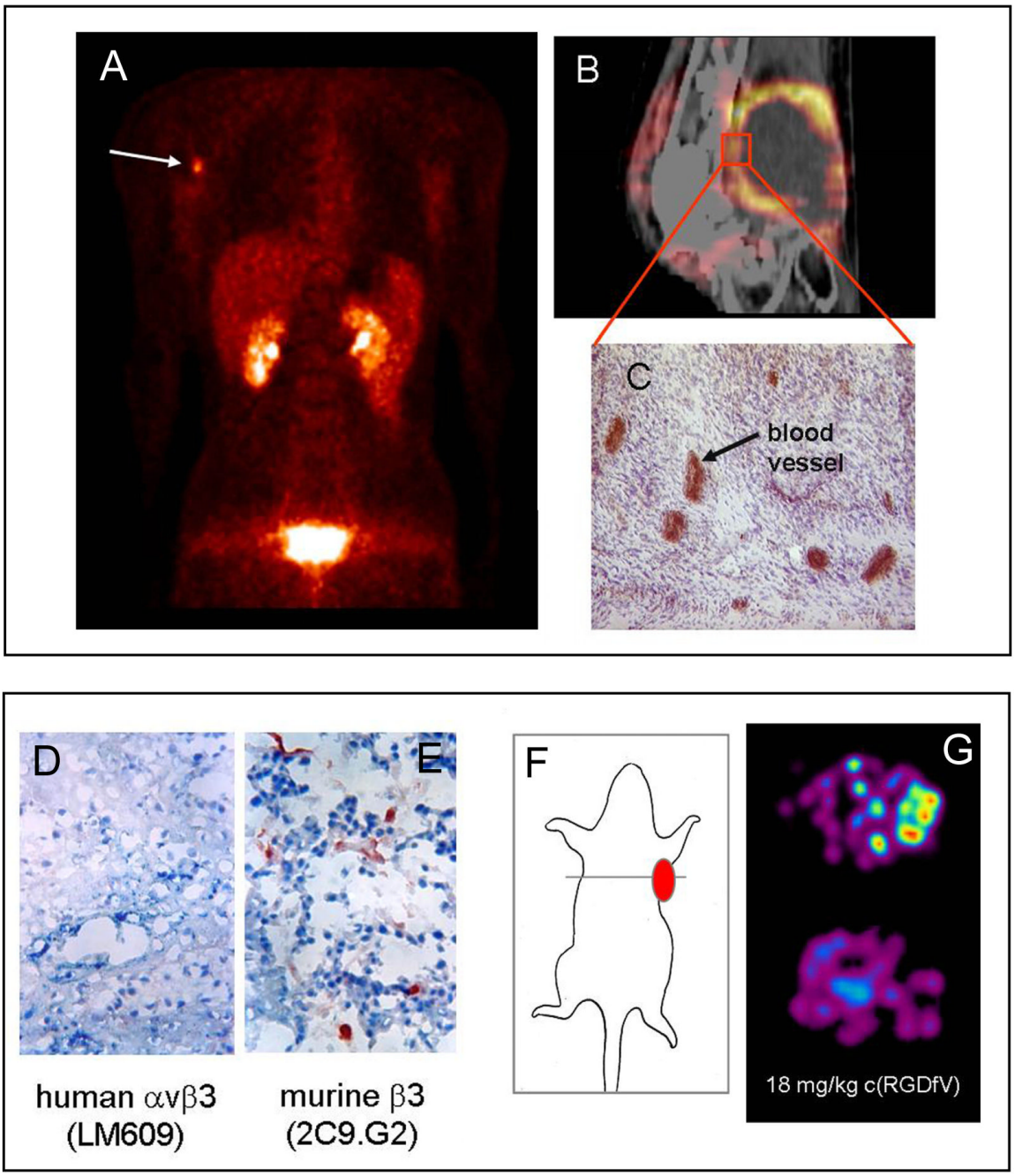

Fig 3. Detection of neoangiogenesis

Upper panel: (A) Coronal image section from a ^{18}FGalacto-RGD PET of a patient with a malignant melanoma and a lymph node metastasis at the right axilia obtained 60 min after tracer injection. The image shows a clearly contrasting tumour and rapid predominately renal elimination with low background activity in almost all areas of the body. (B, C) Patient with a soft tissue sarcoma dorsal of the right knee joint. (B) The image fusion of the ^{18}FGalacto-RGD PET and the corresponding CT scan shows that the regions of intense tracer uptake correspond with the enhancing tumour wall, whereas the non-enhancing hypodense centre shows no tracer uptake. (C) Immunohistochemistry of a peripheral tumour section using the

anti-$\alpha_v\beta_3$ monoclonal antibody LM609 demonstrates intense staining predominantly of tumour vasculature.

Lower panel: (D) Immunohistochemical staining of tumour sections using the anti-$\alpha_v\beta_3$ mAb LM609 demonstrates that the squamous cell carcinoma of human origin do not express the $\alpha_v\beta_3$ integrin. (E) In contrast, staining of sections with an antibody against the murine β_3-subunit indicates that the tumour vasculature is $\alpha_v\beta_3$-positive. (F, G) Transaxial images of nude mice bearing a human squamous cell carcinoma at the right shoulder acquired 90 min after ^{18}FGalacto-RGD injection show a clearly contrasting tumour. The signal reflects tracer accumulation due to $\alpha_v\beta_3$ expression exclusively in the tumour vasculature. Tracer accumulation can be blocked by injecting 18 mg cyclo(-Arg-Gly-Asp-$_D$Phe-Val-) per kilogram mouse 10 min prior to tracer injection indicate receptor-specific accumulation. (figure adapted from Haubner et al. PLoS Med. 2004)

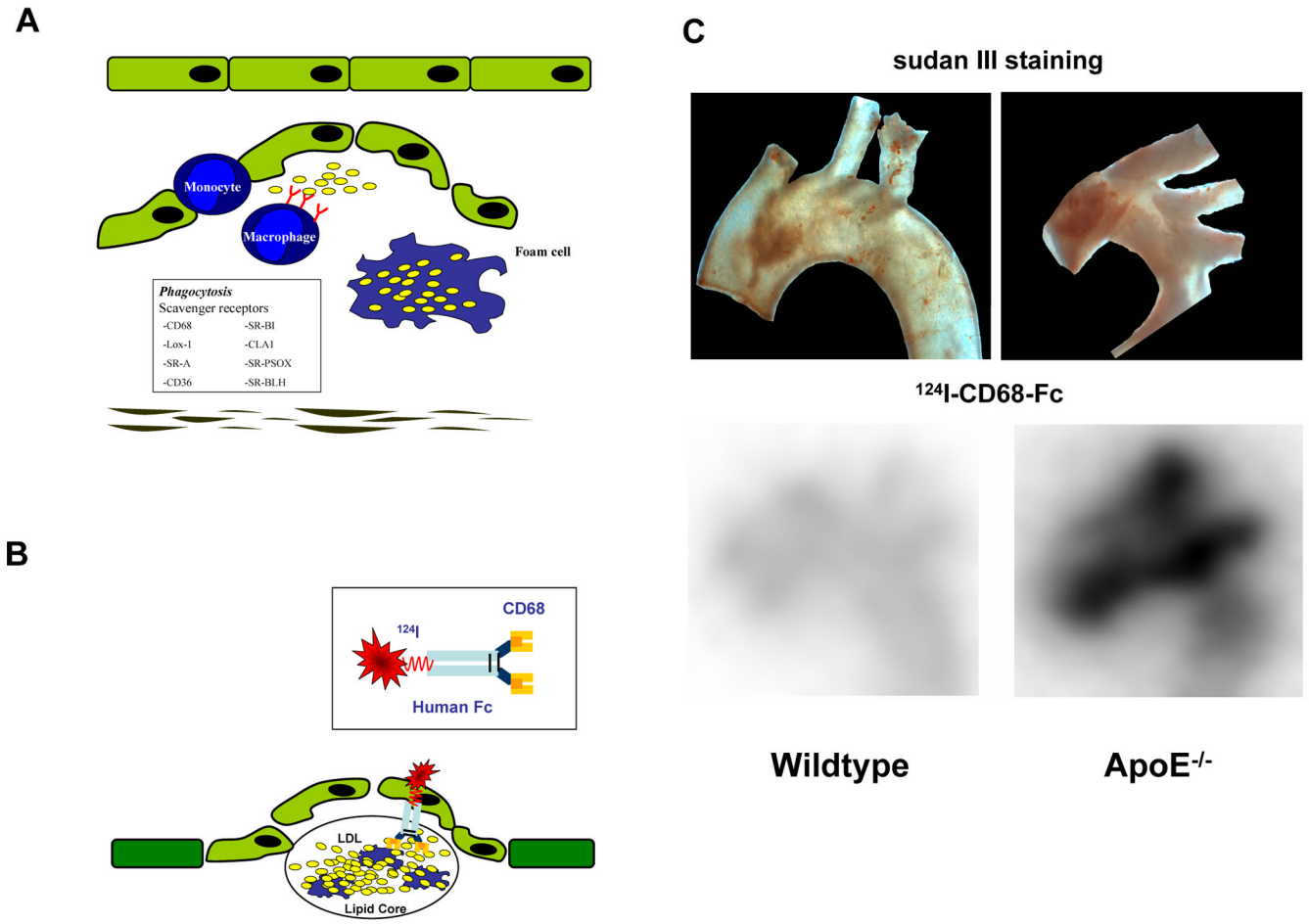

Fig 4. Detection of atherosclerotic plaques by radiolabeled CD68-Fc

(A) (Oxidized) lipoproteins, initiate and sustain the inflammation process in atherosclerotic lesions and are essential for foam cell generation. Scavenger receptors mediate the uptake of lipoproteins into macrophages and, thus, contribute substantially to foam cell formation. (B) A soluble dimeric form of the scavenger receptor CD68 conjugated to an Fc-fragment was radiolabeled with ^{124}I and used to detect atherosclerosis *in vivo*. (C) ApoE −/− or wildtype were fed with a high cholesterol diet for 17 weeks. Subsequently, mice were injected i.v. with ^{124}ICD68-Fc and sacrificed after 48 hours (D) *Ex vivo* nuclear imaging was performed to evaluate tracer activity in the aortic arch. Activity of ^{124}ICD68-FC was enhanced in ApoE −/− compared to wildtype mice (lower panel) and correlated well with plaque extension as shown by sudan red staining in the aortic arch specimen (upper panel).

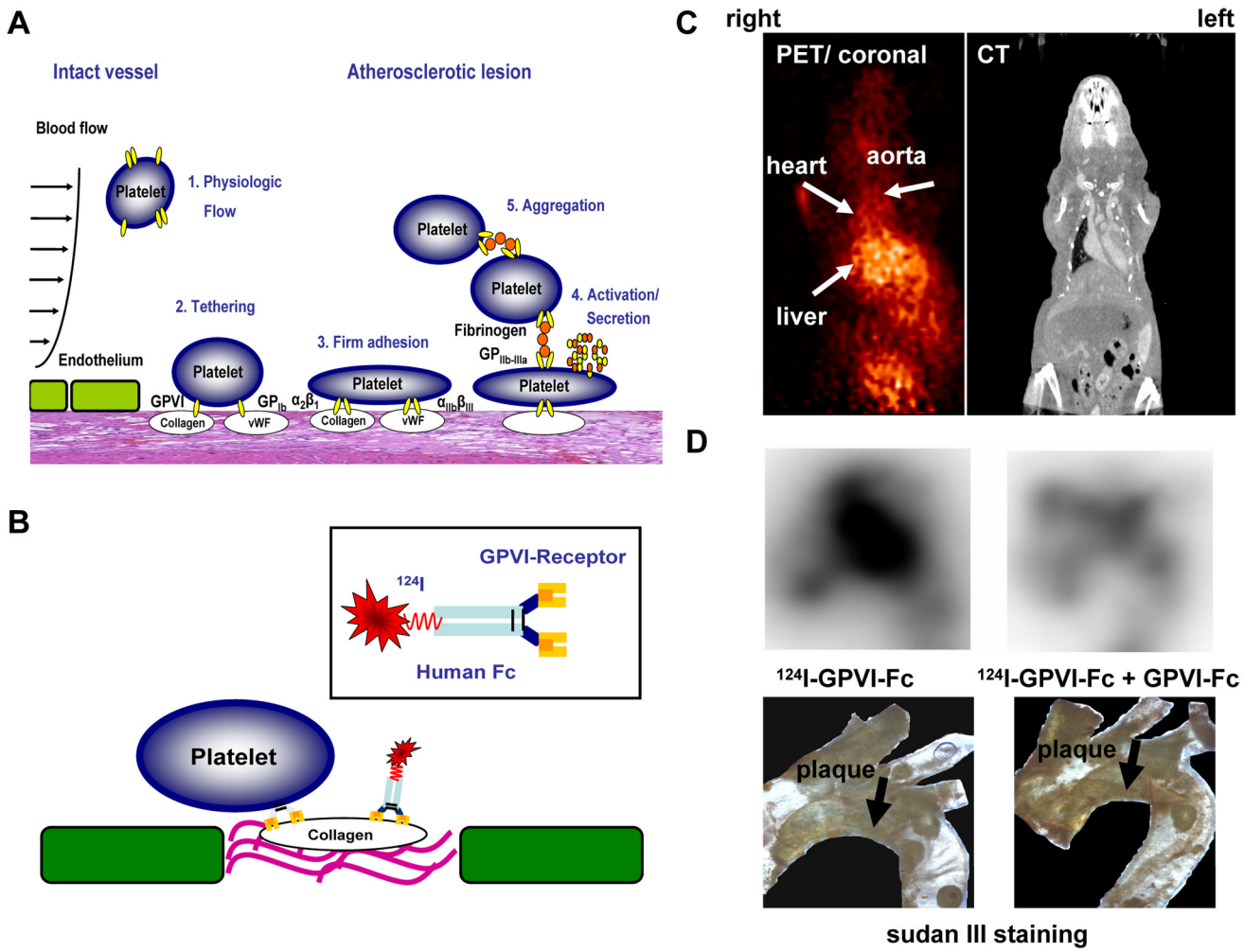

Fig 5. Detection of vulnerable, thrombogenic plaques by radiolabeled platelet GPVI

(A) Pathophysiology of platelet adhesion, secretion and thrombus formation at sites of injured vascular endothelium with exposed extracellular matrix. (1.) Within the intact vessel, platelets do not adhere to the endothelial monolayer under physiological conditions. (2.) At site of atherosclerotic lesions, subendothelial proteins like von Willebrand factor (vWF) and collagen are exposed to blood flow. Platelet adhesion receptors GPIb and GPVI mediate tethering of platelets. (3.) After activation of the integrins $\alpha_2\beta_1$ (collagen receptor) and $\alpha_{IIb}\beta_3$ (fibrinogen receptor), platelets firmly adhere via interaction of these receptors with extracellular matrix proteins. (4.) Subsequently, platelets get activated and secrete distinct mediators resulting in (5.) platelet aggregation via fibrinogen bridges between two $\alpha_{IIb}\beta_3$ receptors and thrombus formation. (B) A soluble dimeric form of human platelet GPVI conjugated to an Fc-fragment was used, which was radiolabeled with ^{124}I. GPVI is essential to establish the first interaction of platelets with an exposed collagen surface. Therefore, we made use of this natural mechanism to detect thrombogenic, and thus, vulnerable plaques. (C, D) ApoE −/− mice were analyzed with ^{124}IGPVI-Fc using an animal microPET scanner (MicroPET Focus 120, Siemens, Germany) (left panel). Images were aquired 24 hours after administration of the tracer and imaging time was 20 minutes. PET images were correlated with CT data (right panel) to verify anatomical structures. (C) shows transverse sections of these experiments. (D) Ex vivo nuclear imaging was performed to evaluate tracer activity in the aortic arch (upper panels). The lower panels show the specimen after staining with sudan III. Activity of ^{124}IGPVI-Fc

correlated well with plaque extension (left panel). The signal could be nearly abolished, when non-labeled GPVI-Fc was injected prior to application of ^{124}IGPVI-Fc. (right panel).

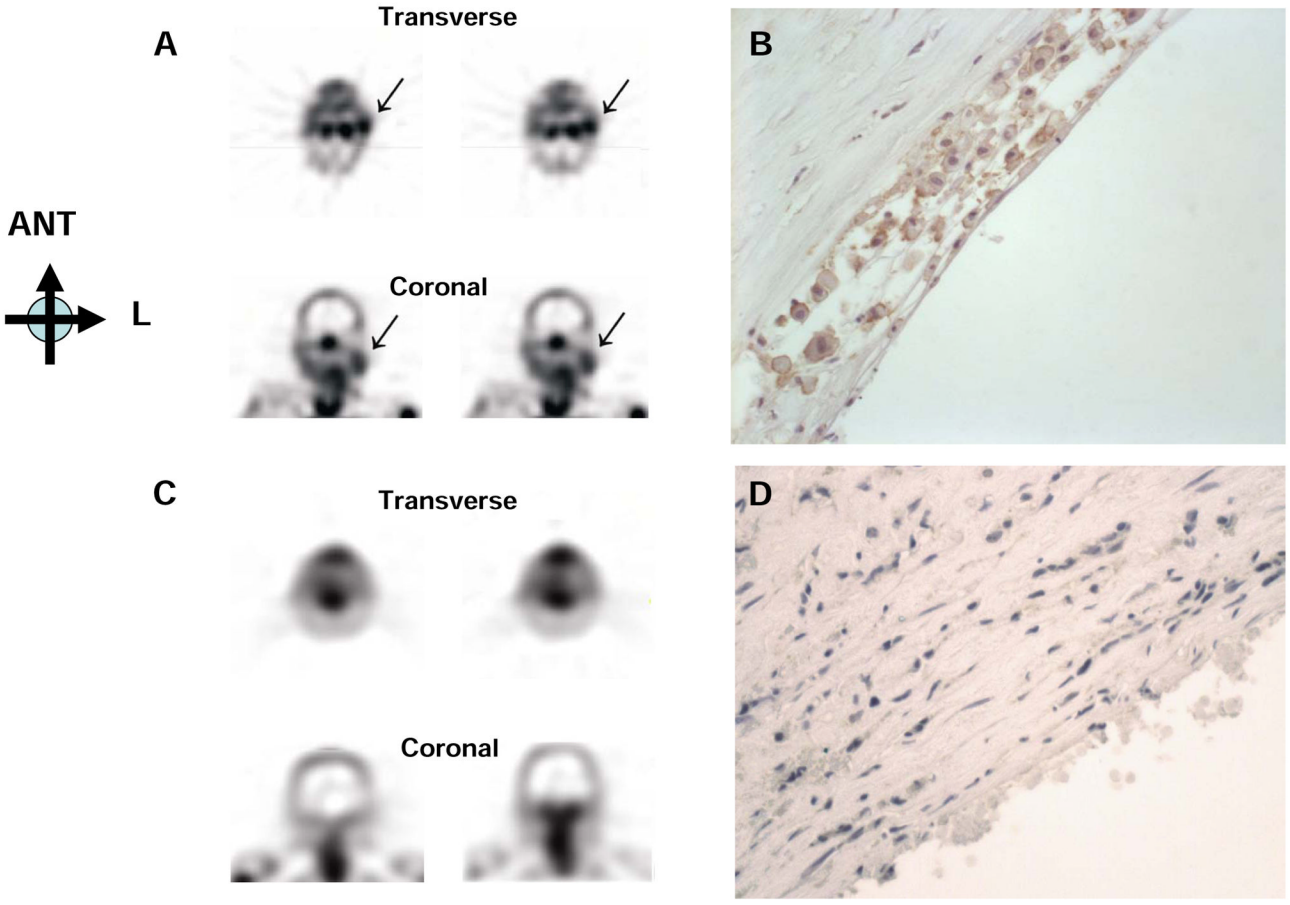

Fig 6. Molecular imaging of apoptosis in atherosclerosis using radiolabeled annexin

^{99m}Tc annexin A5 accumulates in an atherosclerotic lesion in the carotid artery (A, Single-photon emission computed tomography images, ->) of a patient with a recent transient ischemic attack. (B) Annexin A5 in sections of the resected plaque stains strongly in a macrophage-rich area. In contrast, minimal annexin A5 signal (C) appears in the carotid artery of a patient with a remote TI. (D) Annexin A5 immunoreactivity is at a background level in the corresponding smooth muscle cell rich lesion. Images provided courtesy of Dr. Bas Kietselaer and Dr. Leonard Hofstra, University Hospital of Maastricht, the Netherlands. Reproduced by permission from the NEJM.

Tab. 1

Different approaches to visualize atherosclerosis by radionucleide imaging.

Underlying plaque biology	Radionuclide tracer	Experimental setting	Reference
Inflammation	^{99m}Tc-LDL	Human carotid/ ileofemoral artery	Lees at al. 1988 (80)
Lipoprotein accumulation	^{123}I-LDL	Human carotid artery	Virgolini et al. 1991 (45)
	^{125}I-LDL	Rabbit aorta	Virgolini et al. 1991 (46)
	^{99m}Tc-oxLDL	Human carotid artery	Iuliano et al. 1996 (49)
	^{123}I-MDA2 [Ab to oxLDL-epitope]	Rabbit arteries	Tsimikas et al. 1999 (81)
	^{125}I-IK17 [Ab to oxLDL-epitope]	Mouse aorta	Shaw et al. 2001 (82)
	^{123}I-SP4 [Apoliprotein B fragment]	Rabbit aorta	Hardoff et al. 1993 (83)
	^{125}I-SP4	Rabbit aorta	Lu et al. 1996 (84)
Chemotaxis	^{125}I-MCP-1 [chemotactic molecule]	Rabbit aorta	Ohtsuki et al. 2001 (9)
Angiogenesis	^{125}I-c(RGD(I)yV)) [peptide binding $\alpha_v\beta_3$]	Murine ischemic hindlimbs/ HUVECs	Lee at al. 2005 (85)
	^{99m}Tc-(NC100692) [peptide binding $\alpha_v\beta_3$]	Murine ischemic hindlimbs	Hua et al. 2005 (44)
Monocyte recruitment/ activity	^{111}In-monocytes	Human arteries	Virgolini et al. 1990 (17)
	^{18}F-FDG [metabolic activity]	Rabbit iliac artery	Ledermann et al. 2001 (86)
	^{18}F-FDG	Human carotid artery	Rudd et al. 2002 (18)
	^{18}F-FDG	Human arteries	Ben Haim et al. 2004 (87)
	^{18}F-FDG in comparison to ^{18}F-FCH	Mouse aortae	Matter et al. 2007 (22)
	VHSPNKK-modified magnetofluorescent nanoparticel (VNP) [VCAM-1 expression]	Mouse carotid artery	Kelly et al. 2005 (29)
Apoptosis	^{99m}Tc-annexin V [Phosphatidylserine expression]	Rabbit aorta	Kolodgie et al. 2003 (63)
	^{99m}Tc-annexin V	Human carotid artery	Kietselaer et al. 2004 (88)
	^{99m}Tc-annexin V	Swine coronary artery	Johnson et al. 2005 (62)
	^{99m}Tc-annexin V	Mouse aorta	Isobe et al. 2006 (11)
Proteolysis	^{123}I-HO-CGS27023 A [MMP-inhibitor] GHPGGPQGKC-NH_2 [Cathepsin K substrate] – NIRF probe	Mouse aortae and human carotic arteries	Jaffer et al. 2007 (67)
Thrombogenicity and cell recruitment	^{111}In-platelets	Human carotid artery	Minar et al. 1989 (89)
	^{111}In-platelets	Human carotid artery	Moriwaki et al. 1995 (90)
	^{125}I-GPVI/ ^{123}I-GPVI [Platelet collagen receptor]	Mouse carotid artery	Gawaz et al. 2005 (11)

Underlying plaque biology	Radionuclide tracer	Experimental setting	Reference
	^{99m}Tc-DMP-444 [GPIIb-IIIa inhibitor]	Canine coronary artery	Mitchel et al. 2000 (91)
	^{99m}Tc-T2G1s Fab [fibrinogen binding]	Canine femoral/ carotid artery	Cerqueira et al. 1992 (67)
	^{125}I-L19 [fibronectin binding]	Mouse aorta	Matter et al. 2004 (70)